assumption about the spanwise distribution of lift is correct or conservative. Otherwise, the extra margin of the wings will be reduced.

4.4 EMPENNAGE STATIC STRENGTH

Assessment of static strength is much more complex for the Bonanza V-tail than for the wing because of the many issues that arise from imperfect understanding of tail loads, the unconventional empennage configuration, independent strength tests by mod kit suppliers, and the inevitable comparison with the Model 33 Debonair. These issues are addressed in detail in the following sections.

Sections 4.4.1 and 4.4.2 summarize the tail load estimates and strength test results documented in Beech Aircraft Corporation engineering reports. Because of the variety of load conditions, detailed discussion is reserved to follow the summary (Sections 4.4.3 through 4.4.5). The task force has also made calculations to evaluate the uncertainties associated with tail loads in general and their application to the V-tail in particular (Sections 4.4.6 and 4.4.7). A brief discussion in Section 4.4.8 highlights the potential effect of dual controls. Section 4.4.9 discusses potential sources of loads that are considered only implicitly (via the 1.5 factor of safety) in the airworthiness regulations. The available V-tail mod kits are then reviewed, with emphasis on a stub-spar kit for which the best comparative data is available (Section 4.4.10). The task force observations regarding the empennage of the V-tail Bonanza are summarized in Section 4.4.11. Finally, Section 4.4.12 compares the V-tail Bonanza and Debonair tails from the viewpoint of estimated loads and tested strength.

4.4.1. Analysis of Tail Loads

The airworthiness regulations require the analysis of balancing, maneuvering and gust conditions to determine the critical design limit loads for the tail surfaces. CAR 03.2212 through 03.2222 (1946) specify the maneuvering and gust conditions to be considered. Table 4-3 summarizes the conditions considered by Beech[46]. These include the airworthiness requirements and three additional conditions. The "distribution" column in Table 4-3 identifies the type of chordwise load distribution used for each condition (see also Figure 4-9).

CAM 3.171(c) (1954) permits the use of the simplified design criteria specified in Appendix A, CAR 03 for conventional, single engine airplanes with design weights less than 6000 lb. Beech did not use this option to estimate Model 35 tail loads. CAM 3.216(a) (1954) specifies a permissible method to determine the tail load and it allows the use of NACA TN 688[47] or its equivalent when applicable. Beech generally followed the procedures specified in NACA TN 688.

Beech first determined the appropriate equivalent angles of attack and the elevator deflections for the various conditions. The lift coefficients for the tail surfaces for the Model 35 and Models A35 through P35 were then determined based on the data given in NACA TN 688 (1938) for Planform 10 and those for the Models S35 and later were based on Planform 12 (References 32 through 39, 48 through 52). Planforms 10 and 12 are in the shapes of an ellipse and a triangle with rounded corners, respectively. The two planforms have about the same aspect ratio. The total lift on a surface is the product of the lift coefficient, surface area and dynamic pressure. Since NACA TN 688 does not give the lift distribution over the surface, Beech made the following assumptions: spanwise load distribution proportional to

chord length; chordwise distributions in accordance with the certification requirements (Table 4-3). Note that several load conditions were not analyzed for the Model C35. Beech did consider these conditions but did not calculate loads for them. The omission of these load calculations was justified on the basis that these conditions were not critical for the earlier models and, therefore, would not be critical for the C35.

As the gross weight, operating speeds, and engine power increased from 1947 to 1970, Beech made several modifications to strengthen the tail structure. The significant tail modifications are summarized in Section 2 (see Table 2-3, page 10).

Beech determined the critical load for each type of chordwise load distribution for most of the newer models. The critical ultimate loads by model and chordwise distribution that have been calculated by Beech are given in Table 4-4.

During the design of the Model H35, Beech reintroduced Maneuver Condition H to the loads analysis program in a variant identified as Condition G1. Condition G1 differs from Condition H only in the magnitude of the tail load, which was obtained from a chart in CAR 03 instead of NACA TN 688 Planform 10. The Condition G1 load is larger than the corresponding Condition H load.

The history of tail load estimation for the Bonanza series shows that Beech complied with the letter of the airworthiness regulations. However, the case of balancing stabilizer load and unchecked rudder maneuver load has never been required by the regulations and was not considered.

4.4.2 Empennage Strength Tests

The procedures used by Beech to test the Model 35 series empennage were similar to the wing test procedures outlined in Section 4.3.4, including the application of tension patches to simulate the air load distribution. The most extensive testing was performed for Maneuver Condition C (combined unchecked elevator and rudder). There were only limited tests for Condition J (yaw with neutral rudder), Condition G1 (yaw with pro-sideslip rudder) and for Condition A (unchecked elevator). Table 4-5 summarizes the test results in comparison with the corresponding design ultimate loads. The results of other tests performed by mod kit suppliers will be presented and discussed later.

4.4.3 Failure Modes for Conditions A and C

It is important to consider the effect of Condition C on the V-tail in the light of its behavior under Condition A. Recall that Condition A is for full elevator deflection at V_A, while Condition C is for 2/3 elevator and 2/3 rudder. The loads of Condition A are the same on both left and right tails except for a small difference caused by the stabilizer incidence angles for the later models. Conversely, the load magnitudes for Condition C differ greatly because of the differential ruddevator deflections. The maximum load of Condition C on one tail is higher than that of Condition A except for the S35 and later models. Condition A generates a high total tail load which bends the aft fuselage. Conversely, the total tail load of Condition C is much smaller than that of Condition A but has a much larger torque to twist the aft fuselage. Table 4-6 compares the design ultimate loads of Conditions A and C.

TABLE 4-3. CONDITIONS ANALYZED FOR MODEL 35 DESIGN LIMIT TAIL LOADS

35	A35	C35	J35	N35	S35	DISTRIBUTION	CAR 03	DESCRIPTION
A	A	A	A	A	A	1	03.2212(a)	Sudden upward deflection of elevator to maximum position at maneuvering speed
B	B	B	B	B	B	1	03.2212(b)	Sudden downward deflection of elevator to maximum position at maneuvering speed
C	C	C	C	C	C	1	NONE	Unchecked maneuver at maneuvering speed; **combined** up elevator and rudder
D	D		D	D	D	1	NONE	Unchecked maneuver at maneuvering speed; **combined** down elevator and rudder
E	E		E	E	E	1 FOR DOWNLOADS 2 FOR UPLOADS	03.2212(c)	Checked maneuver at **reduced weight**, (forward c.g.) at maneuvering speed and positive load factor of -1.0 for downloads and -3.8 (or -4.4) for uploads
F	F		F	F	F	1 FOR DOWNLOADS 2 FOR UPLOADS	03.2212(c)	Checked maneuver at **gross weight**, (aft c.g.) at maneuvering speed and positive load factor of -1.0 for downloads ; -3.8 (or -4.4) for uploads
G	G	G	G	G	G	1	03.2221(a)	In unaccelerated flight and zero yaw, sudden displacement of rudder to maximum position (limited by pilot effort)
H	H		H	H	H	3	03.2221(b)	15 yaw , rudder deflected to increase yaw, unaccelerated flight (limited by pilot effort)
J	J	J	J	J	J	2	03.2221(c)	Plane yawed 15 , unaccelerated flight, rudder in neutral (limited by pilot effort)
---	K		K	K	K	1 FOR DOWNLOADS 2 FOR UPLOADS	03.2212(c)	Checked maneuver at **reduced weight** critical forward c.g., with positive load factor -1.0, and negative load factor, -4.4
GUST COND.1	GUST COND.1		GUST COND.1	GUST COND.1	GUST COND.1	2	03.2213(a) 03.2213(b) 03.2213(c)	+/- 30 fps gust at cruising speed, flaps retracted (at **reduced weight**, forward c.g., and at **gross weight**, aft c.g.) +/- 15 fps gust at flap speed, flaps extended (at **reduced weight**, forward c.g., **gross weight**, aft c.g.) **1957 AND LATER:** +/- 15 fps gust at dive speed (V_d) (at **reduced weight**, forward c.g., and at **gross weight**, aft c.g.)
GUST COND.2	GUST COND.2		GUST COND.2	GUST COND.2	GUST COND.2	2	03.2222	+/- 30 fps lateral gust at cruising speed in unaccelerated flight
GUST COND.3	GUST COND.3		GUST COND.3	GUST COND.3	GUST COND.3	2	NONE	+/- 30 fps gust normal to one control surface (at **reduced weight**, forward c.g. and at **gross weight**, aft c.g.)

TABLE 4-4. DESIGN ULTIMATE TAIL LOADS

MODEL & SAR	MANEU-VERING CONDITION	LOADS VIA BEECH METHOD	CAR LOADING DISTRIBUTION #	CAR LOADING DISTRIBUTION SHAPE	CAR LOADING DISTRIBUTION #	MODEL & SAR	MANEU-VERING CONDITION	LOADS VIA BEECH METHOD
35 35-9	A B C(23) C(0) G(up) G(down) H(up) H(down) J(right) J(left)	-660 + 242 -759 -182 -660 + 242 -209 -188 + 252 -615	1 3 2	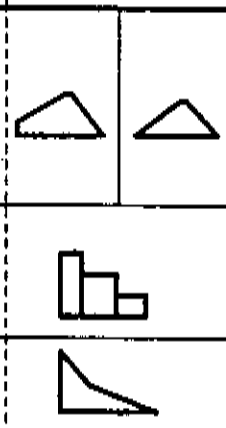	1a 3 2	J35 49-18	A B C(25) C(3) G(up) G(down) H(up) H(down) J(right) J(left)	-893 -417 -998 -312 -744 + 342 -209 -164 + 476 -818
A35 49-9	A B C(23) C(0) G(up) G(down) H(up) H(down) J(right) J(left)	-813 + 251 -881 -276 -735 + 210 -288 -236 + 263 -774	1a 3 2	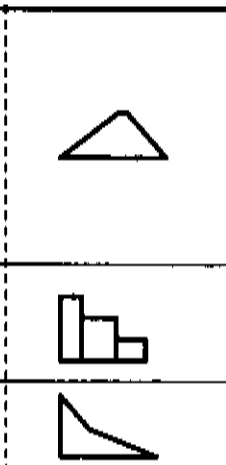	1a 3 2	N35 49-20	A(right) A(left) B(right) B(left) C(21) C(6) G(up) G(down) H(up) H(down) J(right) J(left)	-857 -1017 + 566 + 389 -969 -291 -744 + 323 -291 -65 + 599 -969
C35 49-12	A B C(24) C(3) G(up) G(down) J(right) J(left)	-863 + 374 -983 -297 -744 -312 + 461 -759	1a 2	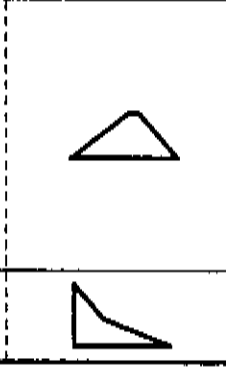	1a 2	S35 49-22	A(right) A(left) B(right) B(left) C(20) C(4) G(up) G(down) J(right) J(left)	-935 -1143 + 398 + 191 + 1040 -345 -882 + 243 + 675 -1247

TABLE 4-5. SUMMARY OF EMPENNAGE STRENGTH TESTS BY BEECH

Model	Condition	DUL (lb.)	Max Load Tested (lbs)
35	C	759	987*(SAR 35-948) 797**(SAR 35-972)
A35	C	881	1057*(SAR 49-910)
C35	C A	998 863	1111* 975(SAR 49-939)
H35	A C	1039 893	1559* 1136+(SAR 49-958)
J35	C	998	998(SAR 49-977)
S35	A	1145**	1261+ (SAR 49-983)
35	J	708	789(SAR 35-972)
C35	J	759	911(SAR 49-939)
H35	J	863	1060+/1036 (SAR 49-958)
J35	J	920	920(SAR 49-977)
S35	J	1247	1247(SAR 49-983)
H35	G_1	722	866(SAR 49-958)
J35	G_1	722	722(SAR 49-977)

*Failure load.
**Failure load for a modified tail, believed not to have entered production.
+ Inferred failure load from test of the S35 in SAR 49-983.
**Based on SAR 49-22 which is different from SAR 49-983.

TABLE 4-6. COMPARISON OF INDIVIDUAL TAIL DUL FOR CONDITIONS A AND C

MODEL	Condition A		Condition C	
	LH	RH	LH	RH
35	660	660	759	182
A35	813	813	881	276
C35	863	863	983	297
J35	-893	-893	-803	491
S35	1143	918	1040	345

The magnitudes and chordwise distributions of these loads have important effects on the tail failure mode. Both conditions use Distribution 1 or 1a, for which the center of loading is located between the front and rear spars. Both spars share the load under these conditions, a fact confirmed by strain gage measurements at the spar roots which showed that the rear spar tensile stress was at least 86 percent of the stress in the front spar[53].

In the test of the production version of the original Model 35, the tail failed in tension at spot welds in the lower flanges of the ribs. The A35 tail failed by crippling in the front spar at WS 35.75 and the rear spar at WS 18.56. Both tests were performed under Condition C, and both failures occurred on the more heavily loaded side. The failure loads were at 130 and 120 percent of DUL of the respective models, i.e., these models possessed ample margins in the empennage structure.

The first major change in tail construction was the introduction of the wide chord in the C35. In order to better understand the significance of the tests and failure modes, however, attention will first be focused on the later Models H35 and S35. The H35 was tested under Condition C. A pre-production version of the S35 was tested under Condition A before the tail was modified and retested to meet its certification requirements.* The pre-production S35 tail contains essentially the same structure as the H35. Therefore, the Condition A test of this tail has been listed under H35 in Table 4-5. In both the Condition A and Condition C tests, the observed failure mode was skin buckling in the aft fuselage followed by tail failure. Under Condition C the final failure was tension at the outboard attachment fastener hole in the front spar root, together with fastener bearing and shearing of one fastener in the rear spar attachments. Under Condition A the final failure was again in the front spar. The failure loads were 150 percent of DUL for Condition C and 127 percent of DUL for Condition A.**

The results of these two tests can be compared because of the similarity in the failure modes. The fact that the failure load for Condition A was much lower than for Condition C (1136 versus 1559 lb.) and the observations of prior fuselage skin buckling suggest that fuselage twisting tended to relieve the bending effect of the asymmetrical Condition C load. Such relief would not occur for actual air loads, however, i.e., one would expect the Condition C margin in-flight to be determined more nearly by the Condition A strength. Taking this ratio from the data in Table 4-6 (1136 lb. strength, 1039 lb. DUL), one would thus estimate the in-flight Condition C margin to be 9 percent rather than the 50 percent found in the Condition C ground test of the H35 tail.

Returning to the Model C35, a similar situation appears in Table 4-5. In this case, both Condition A and Condition C were tested on production C35 tails, and the Condition A failure load is slightly less than DUL for Condition C. This would lead one to believe that the C35 tail might not possess any margin for Condition C. Such a conclusion cannot be clearly drawn, however, because the fuselage failed first in the Condition A test.

---

* The redesign and retesting actually resulted from another test, in which the pre-production S35 tail failed at 85 percent of DUL.

** In a second S35 pre-production test of Condition A, the load reached 140 percent of DUL without failure. The percentages quoted here and in the text refer to DUL for H35.

Another way to assess margin as a function of airplane evolution is to estimate the airspeed at which a maneuver load would exceed the demonstrated strength of the tail. Since aerodynamic loads are involved, the ratio (critical speed $/V_A)^2$ is proportional to the ratio (strength/DUL), and the critical speed can be found. Table 4-7 summarizes this comparison for Maneuver Condition C. The summary suggests decreasing margin from the original 35 to the C35 and improvement thereafter. The data point on the S35 is an artifact of the change from Planform 10 to Planform 12, i.e., the estimate for DUL was increased.

TABLE 4-7. COMPARISON OF CRITICAL AND MANEUVER SPEEDS FOR CONDITION C

Model	Estimated Critical Speed (mph)	Specified Maneuver Speed (mph)	Margin in Airspeed (percent)
35	162	142	14
A35	156	142	10
C35	149	142	5
H35	174	142	23
S35	164	152	8

4.4.4 Failure Modes for Condition J

Condition J (yaw with neutral rudder) uses chordwise Distribution 2, for which the center of load is at WS 36.18 and is more than three inches forward of the front spar. A down load in this case will cause a nose down rotation. This load distribution tends to transfer greater load into the main spar relative to the rear spar. In one test[61] the rear spar root stress was found to be only 67 percent of the front spar root stress (versus 86 percent for Distribution 1/1a).

Of all the Condition J tests, only one tail failed during a test[54]. The tail was a pre-production S35 model which failed through the two outer bolt holes in each spar at a load of 1060 lb., only 85 percent of DUL. The failed tail had essentially the same structure as that of the Model H35, and, therefore, the test result can be compared with other H35 tests, as discussed below. The S35 tail was modified by increasing the gage of the front spar from 0.071 to 0.09 inch and the gage of the rear spar from 0.063 to 0.07 inch. The moments of inertia changed from 1.32 to 1.48 $in.^4$ and from 0.41 to 0.43 $in.^4$, respectively, for the front and rear spars. The modified tail was tested to a load of 1247 lb. (100 percent of DUL) without failure and was used as the production design.

There were no deflection data available for the pre-production S35 tail test, but Mike Smith Aero has tested a Model H35 tail to failure on a jig fixture with limited deflection data[55]. In his test, loads were applied with 50 lb. cement bags to simulate Distribution 2. For loads above 950 lb., the tail experienced severe buckling in the torque box and rapid increase in deflection, especially at the leading edge. For example, the leading edge deflections at the root at loads of 700, 950, and

1000 lb. are 0.1, 0.5 and 0.6 inches, respectively; the corresponding deflections at the tip are 1.6, 4.0 and 5.5 inches (Table 4-10, page 59). The final failure occurred in a sudden collapse at 1150 lb. The failure was characterized by permanent primary box skin buckling and by cracking through the main spar around an upper bolt hole (tension side). One scenario for this failure is that, as the primary box skin buckles (at around 950 lb.), its efficiency in transferring loads between the front spar and the rear spar is reduced. When the skin suffers severe buckling at about 1000 lb., load transfer to the rear spar in the vicinity of the fuselage depends primarily on the root rib, and consequently the main spar must carry a large portion of the load, bending, and torque. The main spar is of open cross section with a relatively low torsional rigidity, and is an inefficient member for carrying a torque. A simple calculation assuming the main spar to develop sufficient stress to carry the total torque (no torque taken by the rear spar) shows that the stress developed would exceed the ultimate strength of the spar material. The combination of the high bending stress and shear stress due to torsion at the root of the main spar led to crack formation at a point on the circumference of the bolt hole. The rapid increase in leading edge deflection after the skin severely buckled is significant for aeroelastic consideration of redistribution of air loads that will be discussed in Section 5.

The above failure scenario does not seem to be applicable to Condition C (Distributions 1/1a) because the center of load is located between the two spars. Even after the skins are buckled, load will still transfer to both spars. The torque can be resisted by the differential loading of the two spars instead of being carried by the torsion of the front spar. In this way, the shear stresses on the main spar due to the torque action of the surface load will not become high after the skin buckles severely, and the surface load can be raised until the main spar fails in bending. Failure would be much more gradual in comparison to the more sudden failure under Distribution 2.

It also appears that the scenario does not apply to the short-chord tail (original 35, A35, B35) because in these cases the center of load for Distribution 2 is between the two spars, like the situation for Condition C.

4.4.5 Tests of Condition G1

Condition G1 (yaw with pro-sideslip rudder) uses Distribution 3, which includes reversed load on the control surface. For the lateral condition being tested, the primary load is increased to 120 percent of its nominal value and the reversed load is 20 percent of the nominal value (CAR 03.222b). This distribution produces about twice as much torque per unit of net load as the other two distributions.

Beech has tested only Models H35 and J35 under Condition G1 as shown in Table 4-5[53,56]. The maximum load tested was 866 lb. (120 percent of ultimate), and no failure occurred. The corresponding torque at the root is 9006 in.-lb.

4.4.6 Issues on Load Magnitude and Distribution

As discussed above, CAR 03 permits the estimation of tail loads by different methods. Beech chose to determine the load magnitude using the data from NACA TN 688. Since there is no single planform given in the NACA Technical Note which is identical to the Model 35 tail, Beech used the data based on Planform 10 or 12 to determine the tail loads for a given angle of attack and elevator deflection. The Model 35 tail has approximately the same aspect ratio as Planform 10 or 12. The data in NACA TN 688 are for the tail alone, i.e., without the influence of wing-

induced downwash, fuselage interference, and propeller swirl. It is uncertain how much influence these effects would have on the load distribution of a V-tail configuration.

Since there are no wind tunnel test or flight survey data to substantiate the load distribution or magnitude for a given condition, the task force examined the estimated loads based on the three methods permitted by CAM 3. The results are shown in Table 4-8. Generally speaking, the load magnitudes obtained by Beech and those from the charts* of CAM 3 are similar. The Condition J loads based on Planform 12 are always higher than those based on Planform 10. The method of Appendix A, CAM 3 gives the highest estimated loads. In fact, the ultimates estimated by the method specified in Appendix A may exceed the ultimate strength of the tail for Models C35 and later.

The basis of the chordwise load distributions specified in CAM 3/FAR-23 is not clear. Presumably the specifications establish conservative estimates, but the presumption is uncertain. To illustrate the uncertainty, the task force considered an example of a two-dimensional airfoil with a movable control surface. The pressure distribution can be expressed in terms of vorticity distributed over the airfoil chord by using thin-airfoil theory for small angles of attack[57].

Figure 4-22 illustrates the results of two example calculations. In both cases the airfoil is at an angle of attack of 10°, while the control surface deflections are +20° for Case 1 and -20° for Case 2.

If the two-dimensional model is considered to be a fin and rudder, then Case 2 is analogous to the situation of a yawed airplane with pro-sideslip rudder (Conditions H and G1). However, the calculated pressure reverses at about one quarter chord. This differs from Distribution 3 which is required for Conditions H and G1.

Also of concern are the unchecked rudder maneuver and rudder-neutral yaw requirements (Conditions H, G1, and J) when applied to a V-tail. As mentioned earlier, the regulations do not require the addition of balancing tail loads for unchecked maneuvers for conventional tails. In the V-tail case however, the balancing elevator load (a vertical load) and the side maneuver loads combine in a ruddevator control system.

If the balancing load is combined with Condition G1 for the Model H35, for example, the torque of the combined load at the tail root is 10250 in.-lb., which exceeds the maximum tested torque of 9006 in.-lb. Whether the H35 tail has margin for this condition is not known, however, because the test article has not been tested beyond the 9006 in.-lb. torque load.

Load distribution is of great importance to the determination of structural strength. Since the accuracy of the distributions on which the V-tail Bonanza design was based have not been confirmed, it is only an assumption that the most critical condition for the structure has been identified.

*These charts are the same as in Appendix B of FAR-23[13].

TABLE 4-8. CRITICAL TAIL DUL ESTIMATES BY DIFFERENT APPROVED METHODS

MODEL, YEAR & SAR	BEECH METHOD		CAM 03/FAR 23 REGULATIONS		LOADING DISTRIBUTION
	NACA #10	NACA #12	APENDIX A	APENDIX B	
(SAR 35-9)	-759	-792	-864	-693	
35	-209	-132	---	---	
(1947-48)	-615	-759	-741	-506	
(SAR 49-9)	-881	-960	-1014	-834	
A35	-288	-315	---	---	
(1949)	-774	-920	-891	-608	
(SAR 49-12)	-983	-1056	-1169	-963	
C35	---**	---**	---	---	
(1951-52)	-759	-1011	-1031	-702	
(SAR 49-18)	-998	-1071	-1245	-1044	
J35	-209	-251	---	---	
(1958)	-998	-998	-1107	-755	
(SAR 49-20)	-1017	-1035	-1332	-1106	
N35	-291	-323	---	---	
(1961)	-1050 ***	-1131	-1193	-813	
(SAR 49-22)	-1125	-1143	-1397	-1164	
S35	-87	-398	---	---	
(1964-65)	-1005	-1247	-1256	-870	

* Balancing tail loads excluded from summary
** No load calculation for **Condition H** done in 49-12
*** Gust loads

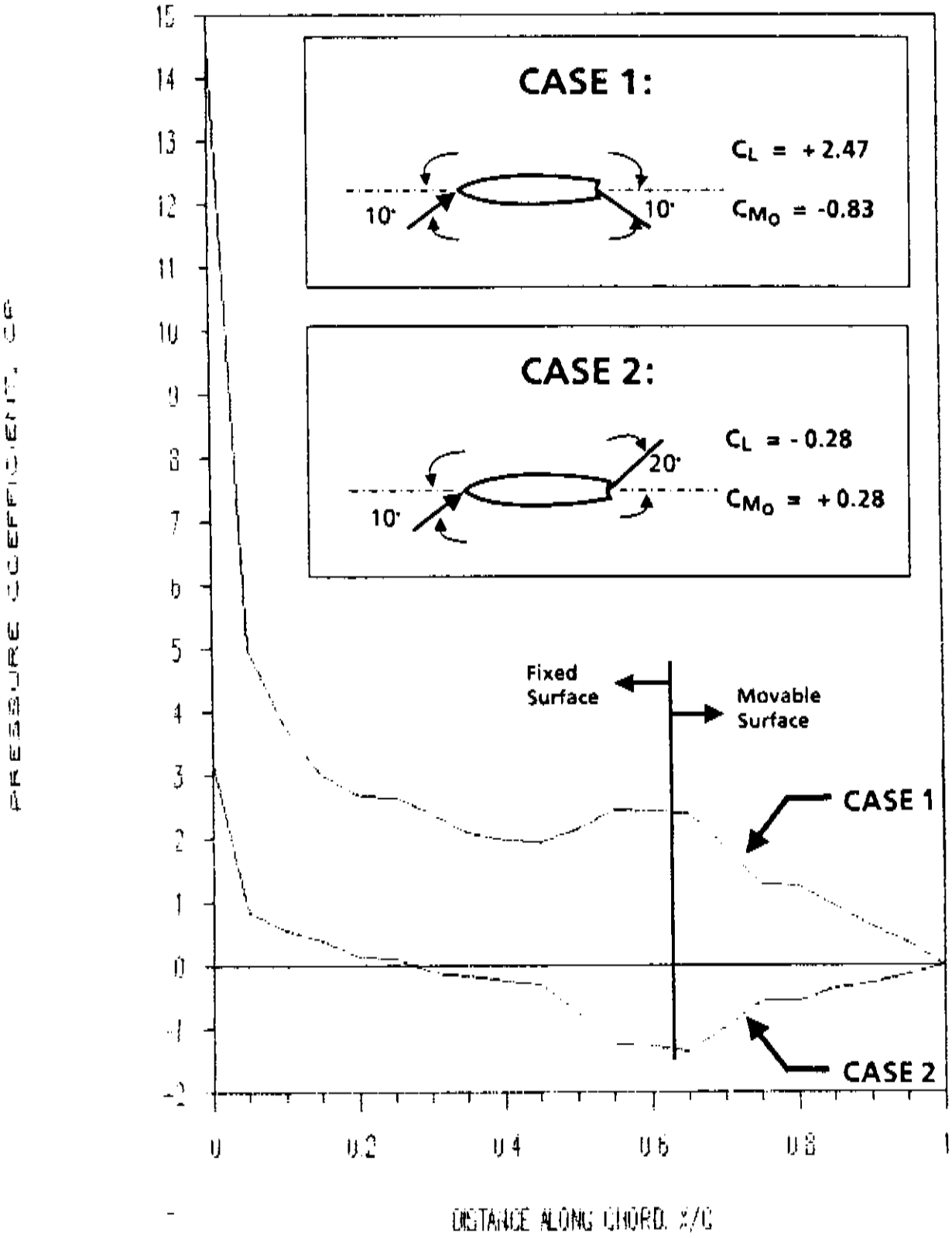

FIGURE 4-22. SAMPLE PRESSURE DISTRIBUTIONS

4.4.7 Estimated Flight Limit Envelope

In the light of the uncertainties in margin associated with discrete-case estimates for tail loads, the task force performed additional calculations to construct flight limit envelopes in terms of operating parameters that are significant for the V-tail. The significant parameters are tail angle of attack, α, ruddevator deflection angle, δ, and airspeed, V.

The envelope speed was estimated by the following procedure. The dynamic pressure

$$q = \frac{L}{1.5\ S\ C_L} \qquad (4\text{-}15)$$

was first calculated for a selected maneuver condition, where L is the tail failure load (lb.) demonstrated in a strength test under the given condition, S is the tail planform area (sq. ft.), and the lift coefficient function $C_L(\alpha, \delta)$ is obtained from NACA TN 688. The factor of 1.5 in Equation 4-14 is the safety factor, i.e., the calculation refers to the limit dynamic pressure rather than ultimate. This is consistent with the way in which the conventional V-n diagram envelope is presented (Figure 4-7). The envelope airspeed is then obtained by solving for V from:

$$V = \frac{\sqrt{2q / \rho}}{1.47} \qquad (4\text{-}16)$$

In Equation 4-15, q is in lb./sq. ft. and ρ= 0.00238 slug/ft3. (sea level air density), V is in ft./sec. The results are converted to mph for presentation (1 mph = 1.47 ft./sec.).

The task force selected the Model C35 under Conditions A, C, and J for this assessment. Figure 4-23 presents the load limit envelopes of airspeed versus ruddevator deflection for two specific angles of attack on the tail, α = -3° and α = -10°. Any point on the figure represents the limit for the parameters indicated, assuming static conditions. The design dive speed, V_D, reflects an operating limit on this plot, just as it does on the V-n diagram. Also shown for reference are the C35 cruise speed, V_C, maneuver speed, V_A, and stall speed, V_S. The ruddevator deflection limit is 23° (2/3 rudder plus 2/3 elevator).

The envelope for α = -10° represents approximately the angle of attack of the trailing tail surface when the airplane has a 15° angle of yaw (Maneuver Condition J). Positive and negative ruddevator deflections for this case correspond respectively to pro-sideslip and counter-sideslip rudder. In the case for 23° counter-sideslip rudder, the limit envelope for α = -10° is exceeded at V_A. Whether or not such a scenario could occur in flight situations involving an inexperienced pilot who overcorrects in an attempt to damp out Dutch roll in turbulent weather has not been established. However, whether or not a typical pilot could physically achieve 23° counter-sideslip rudder at 15° yaw has not been established.

The envelope for $\alpha = -3°$ represents a level flight condition prior to sudden upward elevator deflection for the unchecked maneuver. In this case, possible elevator deflections could exceed the limit envelope at permitted speeds exceeding V_C. One might expect this scenario in unusual flight situations involving panic maneuver attempts to recover from a steep dive or a divergent spiral.

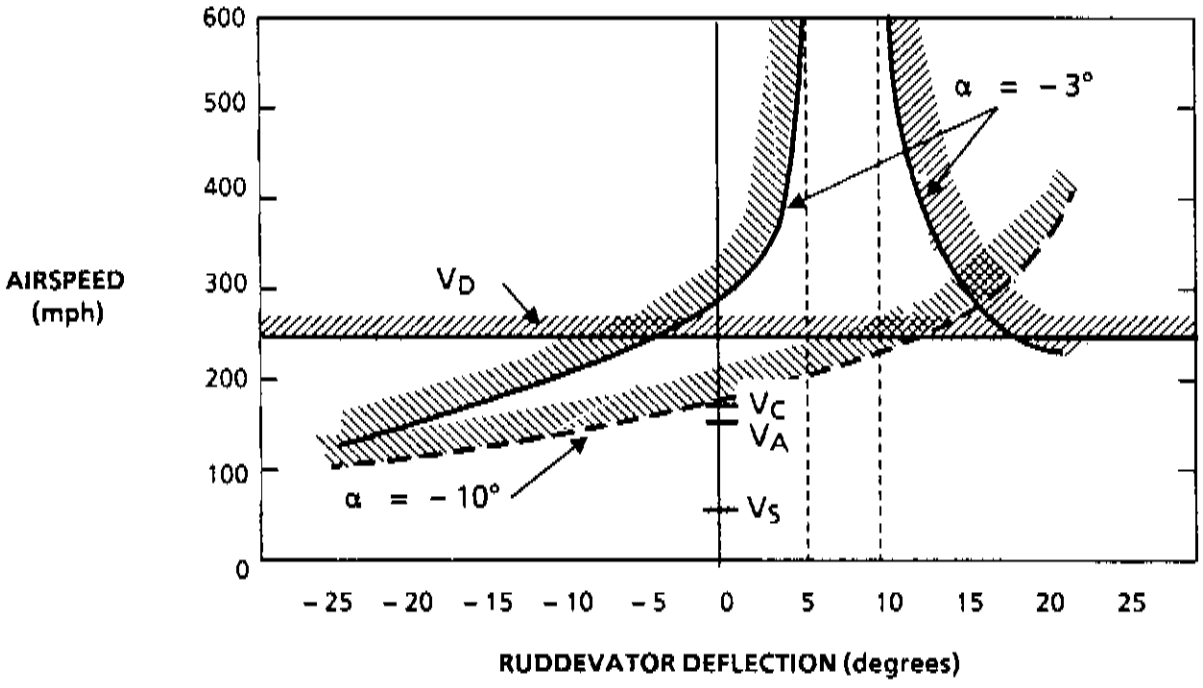

(Flight conditions in the hatched region will exceed the limit tail load. However, the conditions above VD, and those which imply counter sideslip ruddevator at max sideslip, i.e., those shown at $\alpha = -10°$ with negative ruddevator deflection are not required for certification.)

FIGURE 4-23. MODEL C35 TAIL FLIGHT LIMIT ENVELOPES ESTIMATED BY TASK FORCE USING NACA TN-688

The task force also noted that the foregoing observations must be qualified because Figure 4-23 does not reflect the true limits of pilot effort. The 23° ruddevator deflection limit corresponds to a single pilot flying at maneuvering speed, V_A. A single pilot is expected to reach his limit of effort at lower ruddevator deflections when flying at speeds higher than V_A, i.e., the extreme combinations of speed and ruddevator deflection might not be attainable. In addition, the factor of 1.5 will allow 22.5 percent additional velocity before the ultimate load is reached. The counter-sideslip possibility remains of concern, however, and the other scenarios may be attainable in airplanes equipped with dual controls.

4.4.8 Further Consideration of Dual Controls

The production run of the Bonanza series was manufactured with single-pilot controls (wheel on a throw-over yoke). Therefore, single-pilot limit of effort is the only fair way to assess production airplanes at V_A.

However, some Bonanza owners have had their airplanes retrofitted with dual controls. One potential effect of dual-control capability was mentioned in the

preceding section. A second and potentially more serious effect is that a two-pilot effort may be able to develop combined full elevator and full rudder deflection at V_A. The maximum tail load is then limited only by the mechanical stops in the airplane, viz: maximum ruddevator deflection of 35° for all models prior to the S35 and 42° for the S35 and later models. Table 4-9 shows that, although the V-tail strength consistently exceeds DUL for Maneuver Condition C with ⅔ elevator and ⅔ rudder (single-pilot limit of effort), the corresponding DUL estimates for full elevator and rudder, which might be achieved with dual controls, exceed the tail strength in all cases except the Model H35. The dual pilot condition is unusual, however, and the probability of two pilots combining their efforts for maximum deflection is low.

TABLE 4-9. TAIL STRENGTH VERSUS CONTROL SURFACE DEFLECTION

Model	V_A	2/3 Elev and 2/3 Rudder DUL (lb.)	Full Elev and Rudder DUL (lb.)	Failure Load (lb.)
35	130	759	1006	987
A35	142	881	1217	1057
C35	142	983	1280	1111
H35	142	863	1352	1559
S35	152	1040	1856	1261*

*Estimated.

4.4.9 Implicit Phenomena

Three potential sources of load are not considered as specific conditions but are implicitly embodied in the airworthiness requirements via the 1.5 factor of safety on design limit load. The implicit treatment is necessary because the phenomena are difficult to represent by means of discrete load conditions.

The first potential source is a condition of combined maneuver and gust when the airplane is flying at V_A. Such events occur frequently in turbulent weather, but most of the loads involved are so small that even their combinations are non-critical. Conversely, task force calculations have shown that the combination of full elevator and a 30 fps gust would develop a load exceeding the tail strength of the Bonanza. Undoubtedly such combinations could be found for the tails of other airplanes; the crucial question is whether such events occur with any measurable frequency.

The second source is the potential for encountering severe gusts at speeds exceeding V_C. As discussed earlier, the designer is allowed to decrease the gust severity from 30 fps at V_C to 15 fps at V_D (see Section 4.1, and Figure 4-8). This specification implicitly takes advantage of the known statistical properties of air turbulence which suggest that the most severe gusts tend to be centrally located in a turbulent air mass.* Thus, pilots flying above V_C are expected to receive a few warning bumps in time to react by slowing the airplane. This is the typical situation, but there is no guarantee that every pilot will have sufficient warning.

*One well known exception is the leading edge of a thunderstorm cell, where severe vertical gusts may be encountered adjacent to nearly smooth air outside the cell.

The third source is dynamic load amplification factor. If a load is suddenly applied to an elastic structure, the dynamic response may approach twice the amplitude of the static response for the same load. However, since all the applied loads have a finite rise time as compared to the lowest frequency of the structure, the dynamic amplification factor is always less than two. The lowest vibration frequency of the Bonanza tail is about 12 Hertz[56] and 63. The corresponding period is about 0.08 second. Similarly, the torsional vibration frequency of the Bonanza tail is about 40 Hertz[61] and the corresponding period is about 0.025 seconds. If the rise time of any external load is larger than twice the period (about 0.16 second for bending and 0.05 second for torsion) the dynamic amplification factor is less than 1.25[28]. The rise time of any maneuver is expected to be longer than 0.2 second. For example, a snap kick of the rudder to about 7° [67] has a rise time of 0.2 second. Assuming a gust with a velocity variation from zero to peak in 50 ft., the rise time of the gust load for a plane flying at 150 mph is 0.25 second. Thus, the dynamic amplification factors due to maneuver and gust are likely to be less than 1.35.

4.4.10 Stabilizer Modification Kits

The stabilizer is attached to the fuselage only at the front and rear spar locations. These locations remained fixed when the Bonanza was evolved to the wide-chord stabilizer. Thus, the C35 and later models have a wide overhang nose section forward of the front spar. The possibility that the overhanging section might be subject to large deformation under high loads led Beech and three independent suppliers to investigate the strengthening effects of modification kits.

Beech first investigated the addition of a stub spar to anchor the nose box forward of the front spar, but concluded that the support had no appreciable effect on the tail strength. This conclusion is based on the test results[61] which showed that the leading edge support had little effect on the surface deflections or stresses. However, Beech's results seem to indicate that the stresses at the root and the surface deflections for all load distributions were generally less for tests without leading edge support than those with it. No explanation was given for these results. Beech's tests were limited to measurement of stress and deflection at loads below the tail strength, i.e., load redistribution at approach to failure with and without the stub spar was not investigated.

Three independent suppliers later developed and tested modification kits, which have received supplemental type certificates from the FAA. Mike Smith Aero developed a stub-spar kit which attaches the stabilizer nose box to the fuselage. The stub spar attaches to the root nose rib and, via a narrow cut through the fuselage, is bolted to a thin plate riveted between fuselage stringers. Smith's company has also developed a less expensive counterpart to the stub spar. Called the "Tail Safe Kit", it consists of two sets of aluminum brackets which, when placed around the leading edge, are riveted directly to the fuselage, thereby not requiring the time-consuming removal of the stabilizers as was the case with the stub-spar kit. Knots 2U developed a set of cuffs which fit around the leading edge and bolt to the fuselage. Like the second Smith modification, the cuffs can be installed without removing the stabilizers. A similar support kit is offered by B & N Industries.

Both Smith and Knots 2U conducted tests of their kits using loads to simulate Condition J. Based on comparative tests, they claimed that their kits increased the stabilizer strength about 24 and 34 percent, respectively, above the unmodified strength. From the failure scenario described previously (Section 4.4.4) it appears that the primary utility of the stub-spar mod is to relieve the load in the front spar

after skin buckling begins. Consider Table 4-10, which relates loads to stabilizer tip and root deflections measured at the leading edge[27]. At 700 lb. the mod attachment has little effect on the displacement at the leading edge of the stabilizer. At 950 lb. the modification apparently prevents the skin of the torque box from severe buckling and takes up some load reducing the transfer of torque to the front spar and the tip deflection is only 1.9 inches. Without the modification, once the skin buckles, front spar failure occurs at an additional load of 200 lb. because the torque is transferred to the front spar. When the mod is attached , however, it helps the front spar carry the torque. Final front spar failure occurs at 1425 lb. in bending.

The stub-spar kit may not have much effect for Condition C loads, or even for Condtion J in the case of short overhang (original 35, A35, and B35). In both cases the center of load is between the front and rear spars, and for the latter case the torque is also much lower than the torque with the long overhang. After buckling, there is no dramatic increase of torque on the front spar in these cases, and the stabilizer can be expected to fail in bending as has been shown by the previously cited condition C tests (Section 4.4.3).

Smith's result appears to be qualitatively in agreement with that of Beech for condition J before the skin buckles severely. As can be seen in Table 4-10, the leading edge deflection at the root is very small at a 700-lb. load because the stabilizer is torsionally stiff prior to buckling. Therefore, the leading edge support has little effect on deflection. Since Beech terminated the test prior to severe buckling[61], it is natural for Beech to have concluded that a stub-spar mod would be ineffective.

TABLE 4-10. STABILIZER DEFLECTION UNDER STATIC TEST LOADS

SURFACE LOAD (lb.)	UNMODIFIED DEFLECTION (in.)		DEFLECTION WITH MOD (in.)	
	TIP (in.)	ROOT (in.)	TIP (in.)	ROOT (in.)
700	1.6	0.1	1.7	0
950	4.0	0.5	1.9	0
1000	5.5	0.6	3.4	0
1150	7.0	0.9	3.5	0

4.4.11 Comments on Tail Strength

Beech has considered all maneuver and gust conditions specified in CAR-03/CAM 3 for development of tail design ultimate loads. The adequacy of the tail strength was demonstrated by full scale tests, or by inference from tests of other models, for Conditions A, C, G1 H, and J. The task force has made several observations based on review of these results.

Both Conditions A and C have the same chordwise load distribution 1 or 1a over the chord. The load magnitude of Condition C on one tail surface is generally higher than that of Condition A, but there is evidence that the tail may fail at a much lower load for Condition A[55 and 62]. In the light of these results, there remains a question of whether the strength observed for Condition C might be an

artifact of the load simulation method. This question cannot be resolved without additional tests.

The load magnitudes of Condition G1 are generally lower than those of the other conditions, but the chordwise distribution of Condition G1 produces the most torque per unit net load. In view of the torsional failure mechanism described in Section 4.4.4, Condition G1, can be still important in the evaluation of the strength. The load magnitude depends on the interpretation of the airworthiness requirements, which are written primarily for conventional tails. At issue is whether or not one should consider the combined balancing loads and lateral maneuvering loads in the design requirements. The combined loads discussed in Section 4.4.5 result in a higher torque than the maximum torque tested by Beech.

In the Beech tests, tension patches were used to apply loads to the skins. Even though the rigidity of the cloth tension patches used by Beech is small, it may influence the buckling strength of the skin, especially at locations where the skin is not structurally supported. The strength of the structure can be affected. Tests should be conducted to establish quantitatively this effect.

CAR 03/CAM 3 permits the use of different methods to determine the tail loads. Some methods give higher loads than others. As shown in Table 4-8, the procedure specified in Appendix A, CAM 3 generally gives the highest load. The tails of some models may not be able to withstand the higher estimated design ultimates. Since the V-tail is an unconventional configuration, in the absence of wind tunnel test or flight survey results, the task force is unable to determine if the lower DUL estimated by the other permissible procedures are conservative.

There exist maneuvers, which, when executed at, or even below, the maneuver speed, can produce loads exceeding the limit load of the tail (Section 4.4.7). Such maneuvers are unlikely under normal circumstances, but inadvertent executions by inexperienced pilots might be possible. The combination of gust and maneuvering loads can also exceed the tail strength. Such combinations are improbable but not impossible.

The leading edge support attachment is expected to increase the tail strength under load Conditions J and G1 for the stabilizer with the long overhang, but it has little effect under Condition C or under any condition for the stabilizer with the short overhang. The failure mechanism of the stabilizer with the long overhang involves a transfer of torque to the front spar after the skin buckles This mechanism may have significant effect in lowering the torsional divergence speed for certain maneuvering conditions (see Section 5).

4.4.12 Comparison with the Model 33 Debonair

The original Model 33 was modified from K35 with primary changes in the tail configurations from the V-tail to a conventional straight tail. The horizontal tail of the Model 33 has a planform and dimensions similar to those of the 35 with the short nose section. The comparison of spar dimensions and moments of inertia is given in Table 4-11.

The available ultimate loads for two Model 33 airplanes and the corresponding Model 35 airplanes are summarized in Table 4-12. Models 33 and K35 are similar in weight and operating speeds, and so are Models C33A and S35. Since no detailed data for the K35 is available, the data for the J35 (which closely resembles the K35)

is used. It is apparent that the Condition C ultimate loads for the corresponding models are approximately equal. The main difference between the two planes lies in the loads for Conditions J and G1, where the Model 35 has much higher design loads than the corresponding models of the 33. The centers of these loads are located forward of the front spar for the models of the 35 with the long nose section. The transfer of torque to the front spar after the stabilizer skin buckles is believed to be a mechanism that leads to the tail failure of the 35 under these loads. For the 33, not only are the load magnitudes much lower but also the load centers are between the two spars and the net torque about the front spar is much smaller. Therefore, in comparison with the 35, the 33 has a much stronger tail.

TABLE 4-11. DIMENSIONS AND MOMENTS OF INERTIA OF STABILIZER SPARS

MODEL	FRONT SPAR GAGE (in.)		REAR SPAR GAGE (in.)		MOMENT OF INERTIA (in^4)	
	SPAR	DOUBLER	SPAR	DOUBLER	FRONT	REAR
35-E35	0.071	0.091	0.051	0.064	1.32	0.35
F35-P35	0.071	0.091	0.063	0.071	1.32	0.41
S35-V35B	0.090	0.091	0.070	0.071	1.48	0.43
33	0.072	0.072	0.050	0.064	1.25*	0.39*
C33A	0.080	0.080	0.072	0.064	1.39*	0.45*

* Includes 0.02 inches thick doubler strips on the top and bottom flanges.

TABLE 4-12. AVAILABLE TAIL DUL FOR THE MODEL 33 AND EQUIVALENT 35 MODELS

MODEL	LOAD CONDITION	HORIZONTAL TAIL (lb.)	VERTICAL TAIL (lb.)	REFERENCE
33	C (1S/17S**) J (4S/19S**) G_1 (III4/18S**)	995 822 -447/128	----	SAR 69-901
J35	C J G_1	982 982 -866/144*		SAR 49-18
C33A	C (1S/17S**) J (4S/19S**) G_1 (III/18S)	1136 945 -527/150*	965 965 -653/109*	SAR 69-908
S35	C J G_1	1143 1247 -866/144*		SAR 49-22

---- not available.
* Load on hinge line.
**Beech designations for the horizontal and vertical tails of the Model 33.